Chronic High-Fat Feeding Affects the Mesenchymal Cell Population Expanded From Adipose Tissue but Not Cardiac Atria

FILIPPO PERBELLINI,[a,b] RENATA S.M. GOMES,[a] SILVIA VIEIRA,[a] DOUGAL BUCHANAN,[a] SOPHIA MALANDRAKI-MILLER,[a] ARNE A.N. BRUYNEEL,[a] MARIA DA LUZ SOUSA FIALHO,[a] VICKY BALL,[a] KIERAN CLARKE,[a] GIUSEPPE FAGGIAN,[b] CAROLYN A. CARR[a]

[a]Department of Physiology, Anatomy and Genetics, University of Oxford, Oxford, United Kingdom; [b]Department of Cardiac Surgery, University of Verona, Verona, Italy

Correspondence: Filippo Perbellini, Ph.D., Department of Physiology, Anatomy and Genetics, Sherrington Building, Parks Road, Oxford OX1 3PT, United Kingdom. Telephone: 4474569296; E-Mail: f.perbellini@imperial.ac.uk

ABSTRACT

Mesenchymal stem cells offer a promising approach to the treatment of myocardial infarction and prevention of heart failure. However, in the clinic, cells will be isolated from patients who may be suffering from comorbidities such as obesity and diabetes, which are known to adversely affect progenitor cells. Here we determined the effect of a high-fat diet (HFD) on mesenchymal stem cells from cardiac and adipose tissues. Mice were fed a HFD for 4 months, after which cardiosphere-derived cells (CDCs) were cultured from atrial tissue and adipose-derived mesenchymal cells (ADMSCs) were isolated from epididymal fat depots. HFD raised body weight, fasted plasma glucose, lactate, and insulin. Ventricle and liver tissue of HFD-fed mice showed protein changes associated with an early type 2 diabetic phenotype. At early passages, more ADMSCs were obtained from HFD-fed mice than from chow-fed mice, whereas CDC number was not affected by HFD. Migratory and clonogenic capacity and release of vascular endothelial growth factor did not differ between cells from HFD- and chow-fed animals. CDCs from chow-fed and HFD-fed mice showed no differences in surface marker expression, whereas ADMSCs from HFD-fed mice contained more cells positive for CD105, DDR2, and CD45, suggesting a high component of endothelial, fibroblast, and hematopoietic cells. Both Noggin and transforming growth factor β-supplemented medium induced an early stage of differentiation in CDCs toward the cardiomyocyte phenotype. Thus, although chronic high-fat feeding increased the number of fibroblasts and hematopoietic cells within the ADMSC population, it left cardiac progenitor cells largely unaffected. STEM CELLS TRANSLATIONAL MEDICINE 2015;4:1403–1414

SIGNIFICANCE

Mesenchymal cells are a promising candidate cell source for restoring lost tissue and thereby preventing heart failure. In the clinic, cells are isolated from patients who may be suffering from comorbidities such as obesity and diabetes. This study examined the effect of a high-fat diet on mesenchymal cells from cardiac and adipose tissues. It was demonstrated that a high-fat diet did not affect cardiac progenitor cells but increased the number of fibroblasts and hematopoietic cells within the adipose-derived mesenchymal cell population.

INTRODUCTION

Heart diseases are the number 1 cause of death globally, and 65% of the people affected by type 2 diabetes suffer from some form of heart disease or stroke. Considering that the number of people with diabetes is increasing and that it has been estimated that by 2030, 552 million people will have diabetes [1], there is an urgent need for the development of a novel approach to treatment of advanced and terminal heart failure. In the past few years, cell-based therapies have emerged as promising strategies that aim to replace cardiomyocyte loss after myocardial injury. Various cell types have been used clinically with the aim of heart repair [2–4]. The implantation of these cells has shown positive effects, mostly through paracrine mechanisms; however, the complete differentiation and integration of donor cells in the myocardium is limited and still under debate [2–4]. Therefore, to improve current therapies, it is important to know what type of cells are used and select the most effective cell types. Type 2 diabetes mellitus (T2DM) is a metabolic disorder that alters the composition of plasma metabolites, and therefore the heart and

the other tissues have to adapt to a different availability of carbohydrates, free fatty acid (FFAs), and ketone bodies to work properly. In addition, tissues become insulin-resistant, resulting in a loss of regulation of adipose tissue lipolysis, which, joined with increased levels of fatty acid transporters on the cell membrane [5], result both in an increase in fatty acid metabolic pathways and β-oxidation of FFAs [6, 7] and in an alteration in tricarboxylic acid cycle flux [8–10]. In association with these metabolic disorders, several studies have demonstrated that hypercholesterolemia, diabetes, and hypertension impair the number and function of various progenitor cells [11, 12]. In the past few years, autologous cardiosphere-derived cells (CDCs) and adipose-derived mesenchymal cells (ADMSCs) have been used for preclinical and clinical trials, which have confirmed early short-term safety and therapeutic efficacy [13, 14]. However, because of reduced functionality or a different composition of cell populations, in diabetic patients, the autologous origin of the cells could be a limiting factor for cell transplantation. Here we investigated the functionality and differentiation capacity of ADMSCs and CDCs isolated from mice fed a high-fat diet (HFD).

MATERIAL AND METHODS

Animals and Mouse Model of Diabetes

Animals were obtained from a commercial breeder (Harlan, Oxon, U.K., http://www.harlan.com) and kept under controlled conditions of temperature, light, and humidity, with ad libitum access to water and chow. All the procedures involved in this study were reviewed and approved by the Institutional Animal Care and Use Committee and the Home Office and conformed to the U.K. government regulations (Home Office license 30/2755). For 4 months, 6-week-old wild-type male C57BL/6 mice (20–25 g; n = 24) were fed HFD (Special Diet Service, Witham, U.K., http://www.sdsdiets.com) that had an Atwater fuel energy (AFE) of 5.1 kcal/g, comprising 5% from carbohydrate, 35% from protein, and 60% from oil. Control mice (20–25 g; n = 24) received standard chow (Rat and Mouse No.1 Maintenance; Special Diet Services) that had an AFE of 3.3 kcal/g, comprising 75% from carbohydrate, 17.5% from protein, and 7.5% from oil. Because in young and old mice differences in gene expression, metabolism, and atherosclerosis have been noticed in response to diet [15], all mice were sacrificed at a similar time point after 4 months of their allocated diet. At the time of sacrifice, fasted mice were weighed and terminally anesthetized with isoflurane to allow tissue removal. Heart ventricles and the liver were removed and freeze-clamped. Plasma was separated by centrifugation and stored at −80°C. Plasma glucose was analyzed using an ABX PENTRA 400 (Horiba ABX, Montpellier, France, http://www.horiba.com). Plasma nonesterified fatty acids (NEFA) were analyzed using a NEFA assay kit (Wako Chemicals, Neuss, Germany, http://www.wako-chemicals.de). Insulin was measured by enzyme-linked immunosorbent assay (ELISA; Mercodia, Uppsala, Sweden, http://www.mercodia.com). The atria, previously dissected away from ventricles, and inguinal adipose tissues were used immediately for cell isolation.

Cells Isolation and Expansion

Mouse atria were minced and digested in 0.05% trypsin (Invitrogen, Carlsbad, CA, http://www.invitrogen.com) for 3 minutes at 37°C. The small tissue segments were plated out onto fibronectin-coated (Sigma-Aldrich, St. Louis, MO, http://www.sigmaaldrich.com) 60-mm Petri dishes containing complete explant medium

(CEM; supplemental online Table 1). Explants were then cultured at 37°C in 5% CO_2, and medium was replaced every 3–4 days. After a few days, cells with various morphologies, termed explant-derived cells (EDCs), started to emerge from edges of adherent explants and to grow as a monolayer on the fibronectin-coated dish. These cells were harvested once 70%–80% confluent by washing explants with phosphate-buffered saline (PBS; Sigma-Aldrich) followed by 0.53 mM EDTA (Versene; Invitrogen) and then treated enzymatically with 0.05% trypsin for 5 minutes at 37°C. EDCs were resuspended in a growth factor/cytokine-enriched medium named cardiosphere growth medium (supplemental online Table 1) and seeded onto 24-multiwell plates precoated with poly-D-lysine (Sigma-Aldrich; 16.7 μg/ml) at a concentration of 33,000 cells per well. After approximately 4 days, fully formed, loosely adherent cardiospheres were harvested by gentle pipetting and plated in CEM onto fibronectin-coated flasks for expansion as CDCs to passage 2 or 3. The process is illustrated in Figure 1A.

The freshly isolated inguinal adipose tissue was collected into a sterile tube, and the milliliters of tissue were measured. The tissue was minced and then digested with 0.075% collagenase type 2 (Sigma-Aldrich) in PBS for 1 hour at 37°C. The sample was passed through a 100-μm cell strainer (Thermo Scientific, Pittsburgh, PA, https://www.fishersci.com) and centrifuged at 2,300 rpm for 3 minutes so the mature adipocytes were separated from the stromal components. The pellet, known as stromal vascular fraction (SVF), was resuspended in Dulbecco's modified Eagle's medium (DMEM)/F-12 with 20% fetal bovine serum (FBS) and 1% penicillin/streptomycin, and the cells were plated onto 75-cm^2 culture flasks at a density of 20,000 cells per cm^2. ADMSCs were cultured at 37°C in 5% CO_2, and medium was replaced every 3–4 days. The cells were expanded and, once they reached confluence, harvested with 0.05% trypsin and split at a ratio of 1:3. The process is illustrated in Figure 1C. Cell proliferation was assessed by seeding a certain number of cells and trypsinizing these cells once they reached confluence. Doubling time, measured in days, was calculated according to the following equation:

$$T_d = (t_2 - t_1) * \frac{\log(2)}{\log\left(\frac{q2}{q1}\right)}$$

where $t_2 - t_1$ is the number of days between seeding and trypsinization, q_2 is the number of confluent cells, and q_1 is the number of cells seeded initially.

Cardiomyocyte Differentiation

Twenty thousand cells per cm^2 were seeded in a 6-well plate precoated with 0.1% gelatin. Once cells reached confluence, cardiomyocyte differentiation was induced using the two protocols illustrated in Figure 2A and described below. At the end of the treatment the cells were lysed for RNA isolation (Qiagen, Hilden, Germany, http://www.qiagen.com).

TGFβ Conditioned Medium

The cells were treated according to Smits et al. [16] with minor modification. In brief 5 μM 5-azacytidine (Sigma-Aldrich) was added to the differentiation medium (CDM; supplemental online Table 1) in each well; after 6–8 hours, the medium was changed with fresh medium containing 5 μM 5-azacytidine. On each of the next 2 days, 40 μl of 5-azacytidine was added directly
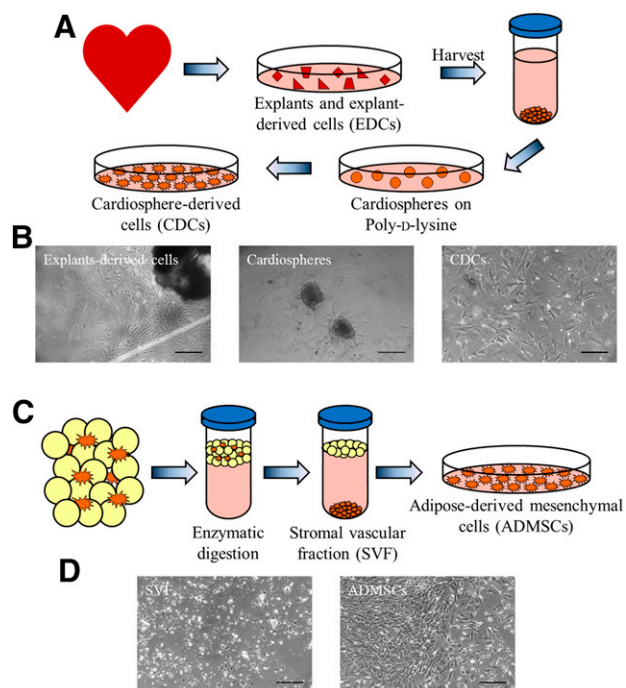
Figure 1. Schematic representation of CDC and ADMSC isolation process and cell morphologies. **(A, B):** Mouse atria were minced, and the small tissue segments were plated out onto fibronectin-coated dishes. EDCs started to emerge from the edges of adherent explants and to proliferate as a monolayer on the fibronectin-coated dish. These cells were harvested and cultured as cardiospheres for a few days. The cardiospheres were then plated onto fibronectin-coated flasks for expansion as CDCs. **(C, D):** The inguinal adipose tissue was minced and enzymatically digested to separate the adipocytes from the stroma. The SVF was then seeded in culture flasks and grown to confluence. Scale bar = 200 μm. Abbreviations: ADMSCs, adipose-derived mesenchymal cells; CDCs, cardiosphere-derived cells; EDCs, explant-derived cells; SVF, stromal vascular fraction.

to the wells, and the differentiation medium was refreshed at day 4. Two days after finishing the 5-azacytidine stimulation, 1×10^{-4} M ascorbic acid and 1 ng/ml transforming growth factor β (TGFβ) (PeproTech, Rocky Hill, NJ, http://www.peprotech.com) were added to the medium. From this point forward, ascorbic acid and TGFβ were added, respectively, every 2 days and 2 times a week.

Noggin Conditioned Medium

The cells were treated according to Jumabay et al. [17] with a modified protocol. Noggin (100 ng/ml) (PeproTech) was added to the differentiation medium and added to each well. After 3 days, medium was removed, and Methocult (M3534; StemCell Technologies, Vancouver, BC, Canada, http://www.stemcell.com) + 100 ng/ml Noggin was added to the cells. On day 8, 2 ml of CDM + Noggin was added to each well, and on day 12, the medium was removed, and 2 ml of fresh CDM + Noggin was added to each well. The differentiation protocol was stopped after 14 days.

Colony-Forming Unit Assay

One hundred eighty cells per well were seeded into a 6-multiwell plate (20 cells per cm^2). CDCs were cultured in CEM, and ADMSCs were cultured in DMEM/F-12 + 20% FBS. After 14 days, adherent

cells were fixed with 70% ethanol and stained with Crystal Violet. A cluster of cells was considered a colony when it was formed from 30 cells or more. Clonogenic potential was expressed as the percentage number of colonies based on the number of cells seeded.

Migratory Assay: Scratch Wound Assay

Cells were grown to confluence and then scratched with a 200-μl pipette tip. The resulting debris was removed, and images of the closing wound were acquired using an inverted microscope after 0, 2, 4, 6, 8, 12, and 24 hours and analyzed using ImageJ software. The migratory capacity was expressed as the percentage of new surface area occupied by the cells in relation to the area at the previous time point.

VEGF Assay (ELISA)

Cell culture medium was collected after 3 days in culture and frozen immediately ($-20°$C). The protein concentration in the medium was determined using BCA protein assay kit. A 96-well plate was coated with 100 μl per well vascular endothelial growth factor (VEGF) capture antibody (R&D Systems Inc., Minneapolis, MN, http://www.rndsystems.com) overnight. An ELISA was performed according to the manufacturer's instructions.

Western Blotting Analysis

Previously freeze-clamped ventricles and livers were crushed using a pestle and mortar, homogenized, and separated by SDS-polyacrylamide gel (12.5%) electrophoresis followed by electrophoretic transfer of proteins from the gel to a nitrocellulose membrane (Pall Corporation, Timonium, MD, http://www.pall.com) using a semidry transfer cell (Bio-Rad Laboratories, Hercules, CA, http://www.bio-rad.com). The nitrocellulose membranes were blocked in 5% (w/v) dried milk in Tris-buffered saline-Tween and then incubated with primary antibody solution at 4°C overnight, followed by the appropriate horseradish secondary antibody peroxidase-conjugated solution (supplemental online Table 2). X-ray film was exposed to the fluorescent membranes, the films were developed in a compact $\times$4 automatic x-ray developer (X-Ograph Imaging Systems, Stonehouse, U.K., http://www.xograph.com) and analyzed using Un-Scan-It, version 6.1 (Silk Scientific, Orem, UT, http://www.silkscientific.com).

Immunohistochemistry

The cells were fixed with 4% paraformaldehyde (PFA) for 10 minutes at room temperature (RT). To target intracellular markers, the samples were permeabilized with Triton X-100, incubated with blocking solution (2% FBS + 2% bovine serum albumin [BSA]) and with primary antibodies for 1 hour (supplemental online Table 3). After rinsing with PBS, the samples were treated with the secondary antibody for 30 minutes, stained with 4',6-diamino-2-phenylindole, and stored at 4°C. The slides were analyzed using an Olympus FV1000 Fluoview confocal microscope.

Flow Cytometry

Once confluent, cells were trypsinized using 0.05% trypsin at 37°C for 3–4 minutes and fixed with 4% PFA, and 2.5×10^5 to 4×10^5 cells per sample were analyzed using flow cytometry. The cells were incubated in blocking solution (2% FBS + 2% BSA) for 30 minutes at RT, incubated for 1 hour at RT with primary antibody (or overnight at 4°C), washed with PBS to remove the excess antibody,
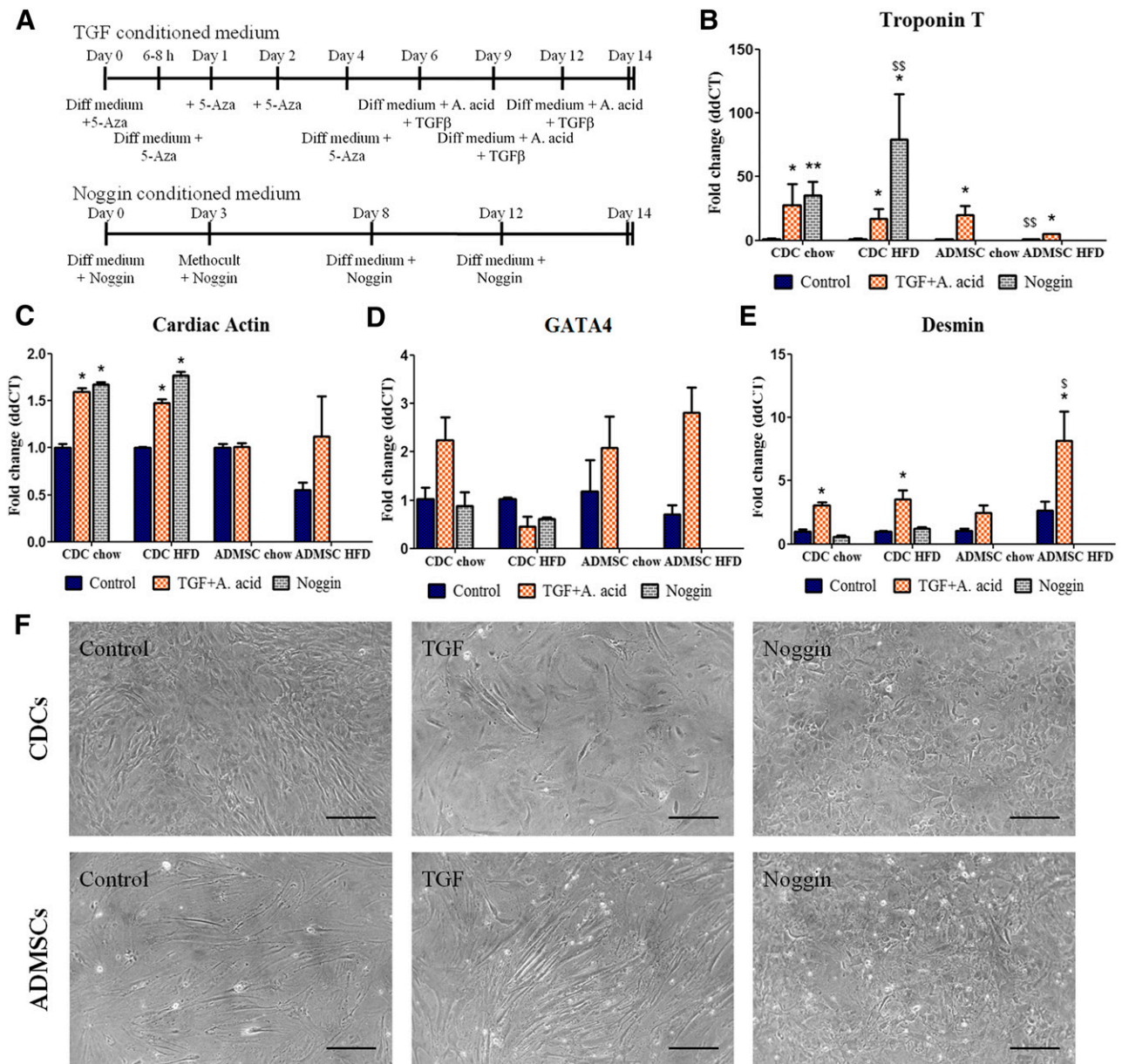
Figure 2. Differentiation of ADMSCS and CDCs. **(A):** Schematic representation of the differentiation protocols. **(B–E):** Relative mRNA expression in differentiated passage 3 ADMSCs and CDCs. All values were normalized to β-actin, glyceraldehyde-3-phosphate dehydrogenase, and β2-microglobulin (CDCs chow-fed, n = 4; CDCs HFD-fed, n = 5; ADMSCs, n = 5). $*$, $p < .05$ vs. control; $, $p < .5$ versus ADMSCs or CDCs chow-fed. **(F):** The differentiation protocols changed the cell morphologies; however, no beating cells were observed in any condition. Scale bar = 200 μm. $*$, $p < .05$; $**$, $p < .01$ (n = 11; statistical analysis is given in supplemental online Table 6). Abbreviations: A. acid, ascorbic acid; ADMSCs, adipose-derived mesenchymal cells; 5-Aza, 5-azacytidine; CDCs, cardiosphere-derived cells; Diff, differentiation; HFD, high-fat diet; TGF, transforming growth factor.

and, if necessary, incubated with secondary antibody for 30 minutes (supplemental online Table 4). The cells were analyzed using a FACSCalibur flow cytometer (BD Biosciences, San Jose, CA, http://www.bdbiosciences.com), and each acquisition included 3–8 $\times 10^4$ events. The data were analyzed using Summit4.3 and Flowing software 2.5.1.

RNA Extraction and Real-Time PCR

Total RNA was extracted using a RNeasy mini kit (Qiagen), according to the manufacturer's instructions. The purity of RNA was quantified with Nanodrop, and the complementary cDNA was generated from 1 μg of RNA using the AB high transcriptase kit

(Applied Biosystems, Foster City, CA, http://www.appliedbiosystems.com). Real-time polymerase chain reaction (PCR) amplification was performed using Applied Biosystems SYBR Green. The polymerase was heat-activated at 95°C for 10 minutes, followed by 40 cycles of denaturation step (95°C for 15 seconds), annealing step (60°C for 30 seconds), and extension step (72°C for 30 seconds). Relative mRNA expression levels were analyzed using comparative Ct methods (the $2^{[minus]\Delta\Delta Ct}$ method) with a normalization to three endogenous controls (the three housekeeping genes: glyceraldehyde-3-phosphate dehydrogenase, β-actin, and β2-microglobulin) and one calibrator (the control sample) (supplemental online Table 5).

Statistical Analysis

Data obtained are expressed as means ± SEM. Differences were investigated using an unpaired t test or a one-way analysis of variance with a Tukey post hoc test and considered significant at $p < .05$ (SPSS software).

Early Diabetic Phenotype

Six-week-old wild-type male C57BL/6 mice (20–25 g; $n = 24$) were fed HFD for 4 months and from the eighth week had a significantly higher mean body weight than chow-fed mice ($p < .01$) (Fig. 3A). Plasma metabolite levels were significantly different between the two groups. High-fat feeding raised fasted plasma glucose, lactate, and NEFA, as well as the fat pad/body weight ratio (Fig. 3B–3E). Insulin levels were also significantly raised in the HFD-fed mice, consistent with a compensatory rise in pancreatic β-cells insulin secretion in response to hyperglycemia. Finally, protein expression was assessed by Western blot on liver and ventricular frozen tissue from chow-fed and HFD-fed mice (Fig. 4A). In liver tissue from HFD-fed mice, pyruvate dehydrogenase kinase 2 (PDK2) and chain acyl coenzyme A dehydrogenase (MCAD) levels were 3.5- and 1.7-fold higher, respectively, than those in tissue from chow-fed mice ($p < .01$; Figs. 4E, 4F). Cardiac PDK4 protein expression was found to be 1.9-fold higher, MCAD levels increased 1.1-fold, and the glucose transporter GLUT4 levels decreased by 22% ($p < .05$; Fig. 4B–4D).

Isolation and Expansion of Cardiosphere-Derived Cells and Adipose-Derived Mesenchymal Cells

At the time of sacrifice, the HFD-fed mice yielded a larger amount of inguinal adipose tissue (3.1 ± 0.5 vs. 1.4 ± 0.4 ml) (Fig. 5A). After collagenase digestion, the cells of the stromal vascular fraction were counted and plated in culture dishes for further expansion or used for experiments (Fig. 1C, 1D). The total number of cells of the stromal vascular fraction of HFD-fed mice was double that from chow-fed mice; however, the number of cells per milliliter was the same (Fig. 5B). At early passages, more ADMSCs were obtained from HFD-fed mice than from chow-fed mice, and the doubling times of ADMSCs of the two groups were estimated to be approximately 10–12 days (Fig. 5C, 5D). EDCs, cardiospheres, and CDCs could be cultured from both chow-fed and HFD-fed mice as illustrated in Figure 1A and 1B. EDCs were harvested, and cell numbers were counted to compare the two diet groups. Cardiospheres did not show any differences in morphology or size whether from chow-fed or HFD-fed mice. Cardiospheres were plated onto a fibronectin-coated surface and grew as a monolayer, giving rise to CDCs that were then expanded to passage 2. The proliferation potential of CDCs was determined by trypsinizing and counting cells (Fig. 5E). The time taken for cardiospheres to become confluent passage 0 CDCs was 7.4 ± 1.3 days when from chow-fed mice and 7.7 ± 1.7 days when from HFD-fed mice. The doubling time of p1 and p2 CDCs was significantly shorter than the time of p0 CDCs, ranging from 4 to 5 days ($p = .01$; Fig. 5F). No significant differences between cells from chow-fed or HFD-fed mice were found in any culture times; however, there was a close inverse correlation between the numbers of EDCs and the SVF, suggesting that the HFD had some effect on the number of EDCs obtained (Fig. 6).

The Effect of the Early Diabetic Phenotype on Cell Yield and Expansion in Culture

The total number of ADMSCs isolated per mouse had a significant positive correlation with plasma glucose and cholesterol and an inverse correlation with lactate levels (Spearman correlation coefficient: glucose = −0.23 $p < .001$; cholesterol = −0.49 $p < .01$; lactate = −0.49 $p < .01$; Fig. 6). Correlations of ADMSC numbers with glucose and lactate were maintained until passage 2 (the Spearman correlation coefficients were, respectively, −0.2 and −0.32; $p < .05$ and $p < .01$), whereas the correlation with cholesterol was lost at passage 2 (Spearman correlation coefficient = −0.14 $p < .08$). EDC numbers correlated with plasma lactate and cholesterol ($p < .05$) but not with glucose; however, these correlations were not seen with CDCs.

Functionality of Cardiosphere-Derived Cells and Adipose-Derived Mesenchymal Stem

To compare the functionality of the two different cell types from the two diet groups, VEGF secretion, clonogenic capacity, and migratory capacity were tested. Biologically active VEGF proteins secreted by ADMSCs and CDCs after plating were measured by ELISA. The assay showed that the same amount of VEGF protein accumulated in the culture medium of CDCs, irrespective of mouse diet. In ADMSC medium from HFD-fed mice, the levels of VEGF were lower, but the decrease was not significant (supplemental online Fig. 2A). ADMSCs were grown to confluence and then scratched with a pipette tip. The surface area of the wounds generated did not differ between the two groups, and the wound closure ratios normalized to the initial area were 17.2% ± 1.5% and 17.7% ± 1.7% for cells from chow-fed and HFD-fed mice, respectively (supplemental online Fig. 2B). It was not possible to perform this experiment with CDCs because of insufficient cell numbers. The clonogenic capacity is usually associated with stemness in cell populations. ADMSCs showed a low clonogenic capacity, mainly yielding two types of colonies, composed of either big or small cells of different morphology (supplemental online Fig. 2C). The clonogenic capacity of ADMSCs from HFD-fed mice significantly decreased over time in culture ($p = .01$). CDCs showed a higher clonogenic capacity (albeit not significantly) that had a trend to increase between passage 0 and passage 2. The colonies varied in cell size, reflecting the heterogeneic nature of the cell populations. No differences were noticed between the clonogenic capacity of cells from the two diet groups.

Phenotypic Characterization of ADMSCs and CDCs From Chow-Fed and HFD-Fed Mice

We assessed the expression of the mesenchymal cell markers CD90 and CD105 and the progenitor cell marker C-kit. In addition we measured the expression of CD45, which is found on hematopoietic cells and mast cells, and the fibroblast marker DDR2. Using flow cytometry, passage 2 CDCs derived from chow-fed and HFD-fed mice were found to contain the same proportions of cells positive for the markers CD45, C-kit, DDR2, CD105, and CD90 (Fig. 7A; supplemental online Fig. 1). In comparison, adipose tissue SVF and ADMSC populations differed between the two groups. A significantly higher expression of CD45-positive cells was noted in the SVF of HFD-fed mice (66.6 ± 1 vs. 58.6 ± 2.1), and this difference was maintained until passage 2 (49.2 ± 7.7 vs. 24 ± 4.8). Furthermore, passage 2 ADMSCs from HFD-fed mice showed significantly higher levels of CD105 (20 ± 4.8 vs. 7 ± 2.5) and DDR2 (7 ± 2.4 vs. 3 ± 0.7) (Fig. 7B, 7C). The results
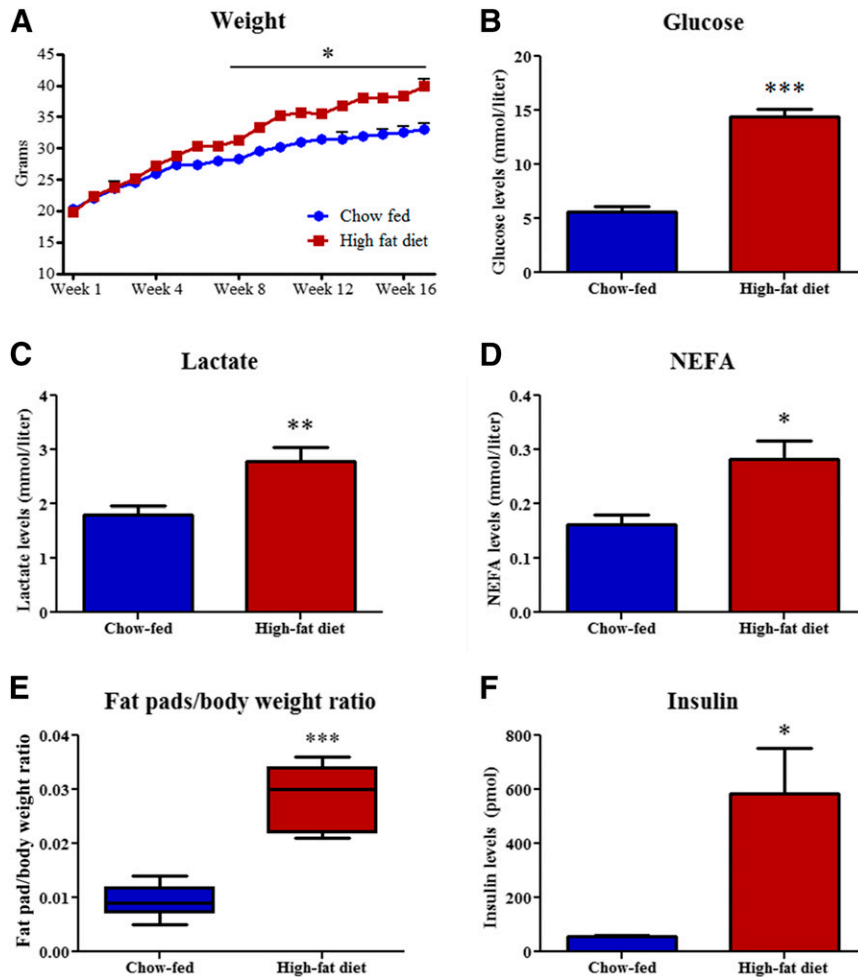
Figure 3. Growth chart and plasma metabolites levels in chow-fed or high-fat diet (HFD)-fed mice. **(A):** For 4 months, 6-week-old mice were fed HFD or chow diet, and from the 8th week HFD-fed mice had a significantly higher mean body weight than chow-fed mice ($n = 24$). **(B–E):** After 4 months of HFD, fasted mice had altered plasma metabolites levels compared with chow-fed mice, and these changes were consistent with an early type II diabetic phenotype. ∗, $p < .05$; ∗∗, $p < .01$ ($n = 6$). Abbreviation: NEFA, nonesterified fatty acid.

confirmed that CDCs and ADMSCs were a mixture of different cell types and revealed their mesenchymal phenotype. Furthermore ADMSCs from the two groups were made up of different proportions of the cell types, demonstrating a higher component of endothelial, hematopoietic cells and fibroblasts in the ADMSCs from HFD-fed mice. Immunocytochemistry of CDCs confirmed what was seen with flow cytometric analysis (Fig. 7D). Some cells were highly positive for CD90 and weakly positive for DDR2, CD45, and CD105. It is worth noting that all the C-kit+ cells were CD45-positive and that C-kit was not expressed on the surface of the cells but was in the cytoplasm with a punctate pattern. Furthermore CDCs displayed a positive staining for the proliferative stem cell markers Oct4 and Sox2.

In Vitro Cardiomyogenic Differentiation Potential of Mouse CDCs and ADMSCs

Both Noggin- and TGFβ-supplemented media were able to induce differentiation in passage 3 CDCs toward the cardiomyocyte phenotype (Fig. 2), significantly increasing mRNA expression of troponin T, cardiac actin, and Gata4. TGFβ-supplemented medium also increased expression of desmin. Although there were no differences in the differentiation potential of CDCs from chow-fed and HFD-fed mice (Fig. 2B–2F), interestingly baseline ADMSCs

from HFD-fed mice showed a significantly lower expression of cardiac actin compared with ADMSCs isolated from chow-fed mice (Fig. 2C). Passage 3 ADMSCs treated with TGFβ-supplemented medium showed some increased expression levels of cardiac differentiation genes; however, ADMSCs from HFD-fed mice seemed to have a slower response to the induction of differentiation. Troponin T, which is increased in differentiation, had a lower expression level in ADMSCs from HFD-fed mice compared with that in cells from chow-fed animals, whereas genes expressed earlier in differentiation (like Gata4 and Desmin) were higher in the cells from HFD-fed mice (Fig. 2B–2E). During the differentiation process, the cells changed morphology (Fig. 2F) but remained positive for the mesenchymal marker vimentin (supplemental online Fig. 4), and no spontaneous beating was observed. Confocal imaging showed very limited expression of troponin T or α actinin in CDCs or ADMSCs after treatment with differentiation medium (supplemental online Fig. 3), indicating that increased mRNA expression had not yet led to any significant protein changes. Actin staining showed increased expression in both CDCs and ADMSCs treated with TGFβ, but not Noggin (supplemental online Fig. 4). Desmin was not detectable in any CDCs, but increased expression was observed in TGFβ-treated ADMSCs (supplemental online Fig. 3).
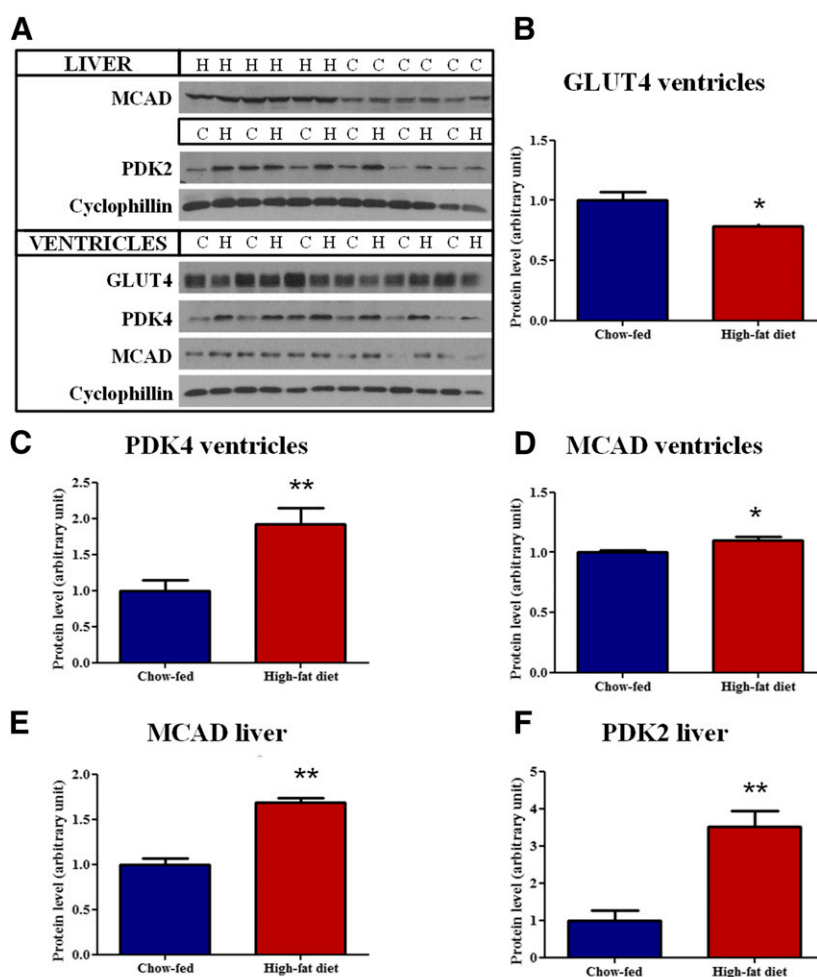
Figure 4. Protein expression in ventricles and livers from chow-fed and high-fat diet (HFD)-fed mice. **(A):** Protein expression was assessed by Western blot on liver and ventricular tissue. **(B–D):** Glucose transporter GLUT4 expression was lower, and PDK4 and MCAD levels were higher in ventricular tissue from HFD-fed mice than from controls. **(E, F):** PDK2 and MCAD levels were higher in livers from HFD mice than chow-fed mice. *, $p < .05$; **, $p < .01$ ($n = 12$). Abbreviations: MCAD, medium chain acyl coenzyme A dehydrogenase; PDK, pyruvate dehydrogenase kinase.

We also observed consistently increased numbers of smooth muscle actin (SMA)-positive cells in CDCs and ADMSCs treated with TGFβ-supplemented medium (supplemental online Fig. 4).

DISCUSSION

In this study, a high-fat diet was used to induce the early diabetic phenotype in the C57BL/6J mouse, which is known to be particularly susceptible to diabetes [18]. Considering that metabolism and the stem cell niches can be affected by age and sex [15], all C57BL/6J mice in the study were male, were randomly allocated to their diets, and were obtained at the same age to eliminate the chance of a selection bias. The advantage of this diet-induced diabetes is that the onset of T2DM takes place in a similar way to that found in Western society—by high caloric intake, leading to obesity in otherwise normal individuals. As such, it might be more relevant to the human condition than other mouse models of diabetes. As a result of this diet, it is clear that metabolic disturbances consistent with early diabetes were achieved, and almost all of the HFD-fed mice had glucose levels within the diabetic range. Consistent with the increase of plasma glucose, greatly reduced cardiac GLUT4 protein levels in

HFD-fed mice would suggest reduced insulin-mediated glucose uptake in their hearts. This reduction was similar to documented levels in db/db mice, which show contractile dysfunction that can be normalized by the overexpression of GLUT4 [19], suggesting that this metabolic disturbance plays a causative role in the cardiac dysfunction seen in diabetes [20]. The increase in MCAD levels in HFD-fed mice is consistent with higher cardiac β-oxidation in high fat-fed animals. Together with the decreased levels of GLUT4, this suggests that a switch in substrate use away from more oxygen-efficient glucose oxidation, toward fatty acid oxidation, had occurred with high-fat feeding [21]. The HFD-fed mice showed increased levels of PDK4 in ventricles and PDK2 in liver, which agrees with other diabetic models and suggests the activation of PDK, by the products of β-oxidation, and inhibition of the pyruvate dehydrogenase complex.

This report has focused on a mouse model of diabetes, which displays most of the hallmarks of early stage of type 2 diabetic pathology and is a satisfactory model for the disease. Cultured ADMSCs and CDCs were examined because of their capacity to improve function in the infarcted heart in animal models [22–25] and because the number of cells attained through in vitro expansion is greater than the number available by direct isolation from digested tissue.
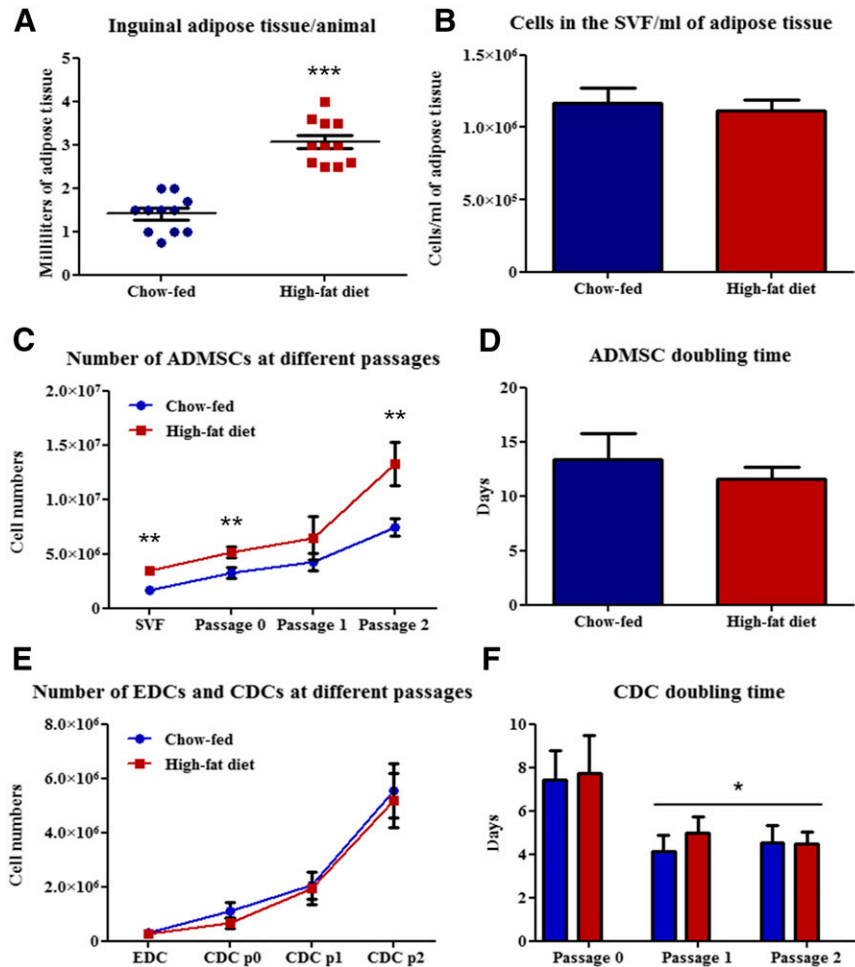
Figure 5. Cell growth rates. **(A, B):** High-fat diet (HFD)-fed mice displayed a larger amount of inguinal adipose tissue on dissection **(A)**, but the amount of cells per milliliter of adipose tissue between the two groups was the same **(B)**. **(C, D):** At early passages, more ADMSCs were obtained from HFD-fed mice than from chow-fed mice **(C)**, but there were no differences in doubling time **(D)**. **(E):** The same number of CDCs were isolated from HFD-fed and chow-fed mice. **(F):** The doubling times of p0–p1 and p1–p2 CDCs were significantly shorter than the time from cardiosphere p0 cells. **(G):** ∗, $p < .05$; ∗∗, $p < .01$; ∗∗∗, $p < .001$ ($n = 11$). Abbreviations: ADMSCs, adipose-derived mesenchymal cells; CDCs, cardiosphere-derived cells; EDCs, explant-derived cells; SVF, stromal vascular fraction.

Although the optimal timing for efficacy remains to be determined, ideally the time in culture would be minimized, because cell administration within a few days of the ischemic event is postulated to help prevent the detrimental long-term changes seen in heart failure, such as cardiac remodeling [26, 27]. Considering that a significant number of patients that could benefit from cell therapy are obese or diabetic, the relative culture time for cells from chow-fed and HFD-fed mice is a relevant determinant of outcome. The doubling time and the proliferation rate of CDCs from chow-fed or HFD-fed animals were the same, which may indicate that the prospect of autologous transplantation for diabetic human patients would not be compromised by a prolonged wait for cells. Hearts from HFD-fed animals were clearly shown to be subject to metabolic disturbances, and the correlation between EDC numbers and plasma lactate and cholesterol also suggests that the diet started to affect the behavior of the cells. However, these differences were not evident beyond the cardiosphere stage, suggesting that diabetic patients with impaired heart energetics would not have an impaired ability to attain cells for therapy.

The increased amount of adipose tissue isolated from HFD-fed mice resulted in a significantly higher number of cells in the SVF

and expanded ADMSCs, which would be a positive factor for an immediate cell selection or a short in vitro expansion. The correlations between plasma glucose, cholesterol, and lactate with the total number of ADMSCs suggest some changes in the adipose tissue. In the past few years, it has been shown that obesity is characterized by the accumulation of diverse immune cells in the adipose tissue. Notably, proinflammatory macrophage infiltration and inflammation-related gene expression precede the development of insulin resistance and appear to be a cardinal feature of obesity in rodents and humans [28, 29]. Our findings, in agreement with others [28–30], showed that ADMSCs from HFD-fed mice had higher levels of CD45+ cells, confirming the infiltration of hematopoietic cells and macrophages in adipose tissue. The next step was to access the functionality of the ADMSCs and CDCs isolated from the two animal groups. It has been shown that metabolic syndromes such as obesity and diabetes can alter the progenitor cell populations and their functionality in various tissues [31, 32]. Pérez et al. [31] showed that though ADMSCs obtained from obese mice and patients were phenotypically similar to controls, they presented differences at the functional level. Emerging evidence suggests that diabetes can also affect the cardiac environment and cardiac progenitor cell populations [33, 34] through an impairment of the growth
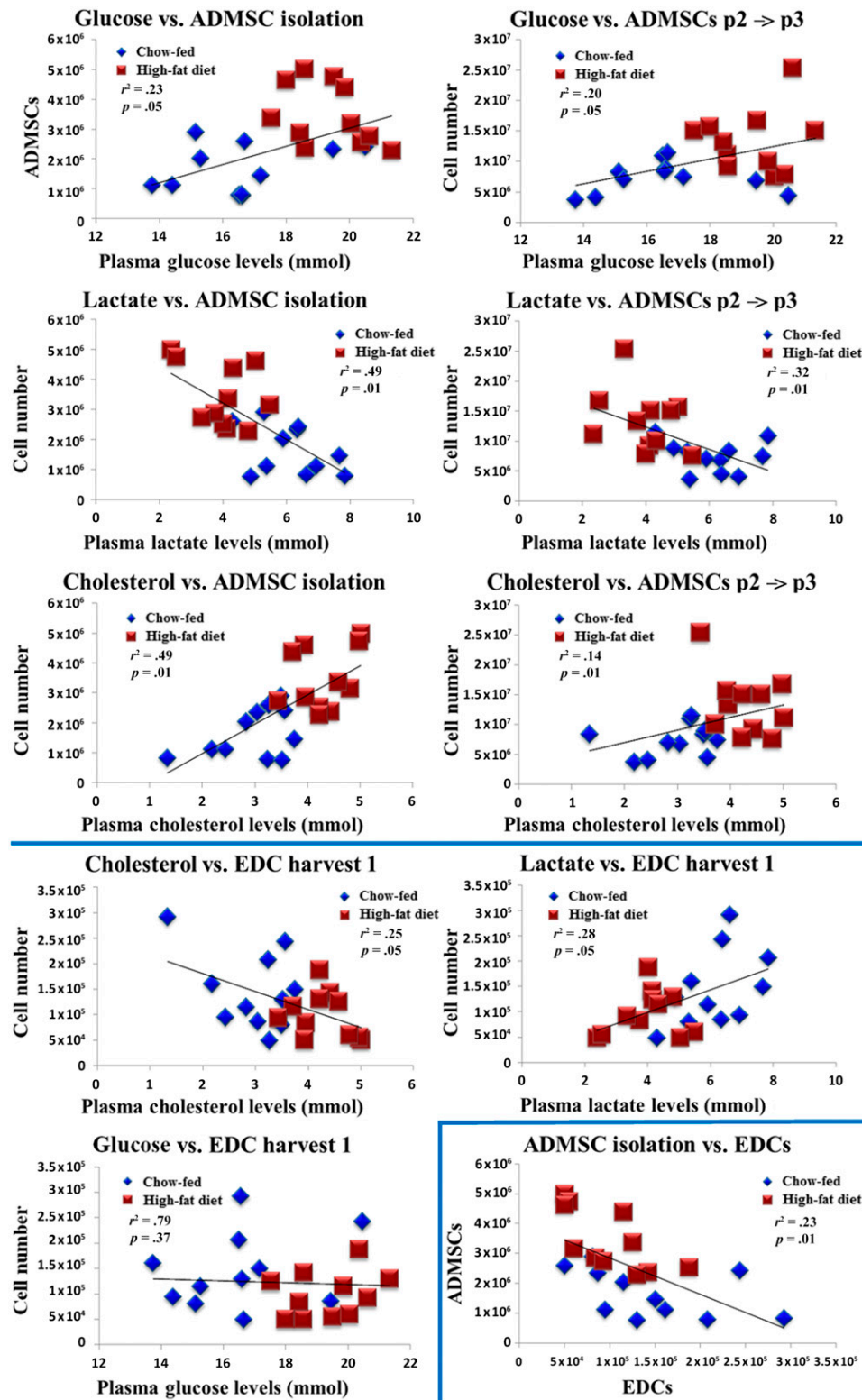
Figure 6. Correlations between cell numbers and plasma metabolites. ADMSC numbers at different passages correlated with plasma levels of glucose, lactate, and cholesterol. EDCs correlated with plasma lactate and cholesterol. A close inverse correlation was noticed between the numbers of EDCs and the stromal vascular fraction ($n = 11$). Abbreviations: ADMSCs, adipose-derived mesenchymal cells; EDCs, explant-derived cells.

reserve of the heart, so that the enhanced cardiac cell death cannot be counteracted by the repopulating myocytes and vascular cells [33, 34]. A fundamental aspect in progenitor cell therapeutic activity is their

ability to release factors that stimulate cell function in both a paracrine and autocrine way. Here we evaluated the biologically active VEGF proteins secreted in the culture media, and we found the same
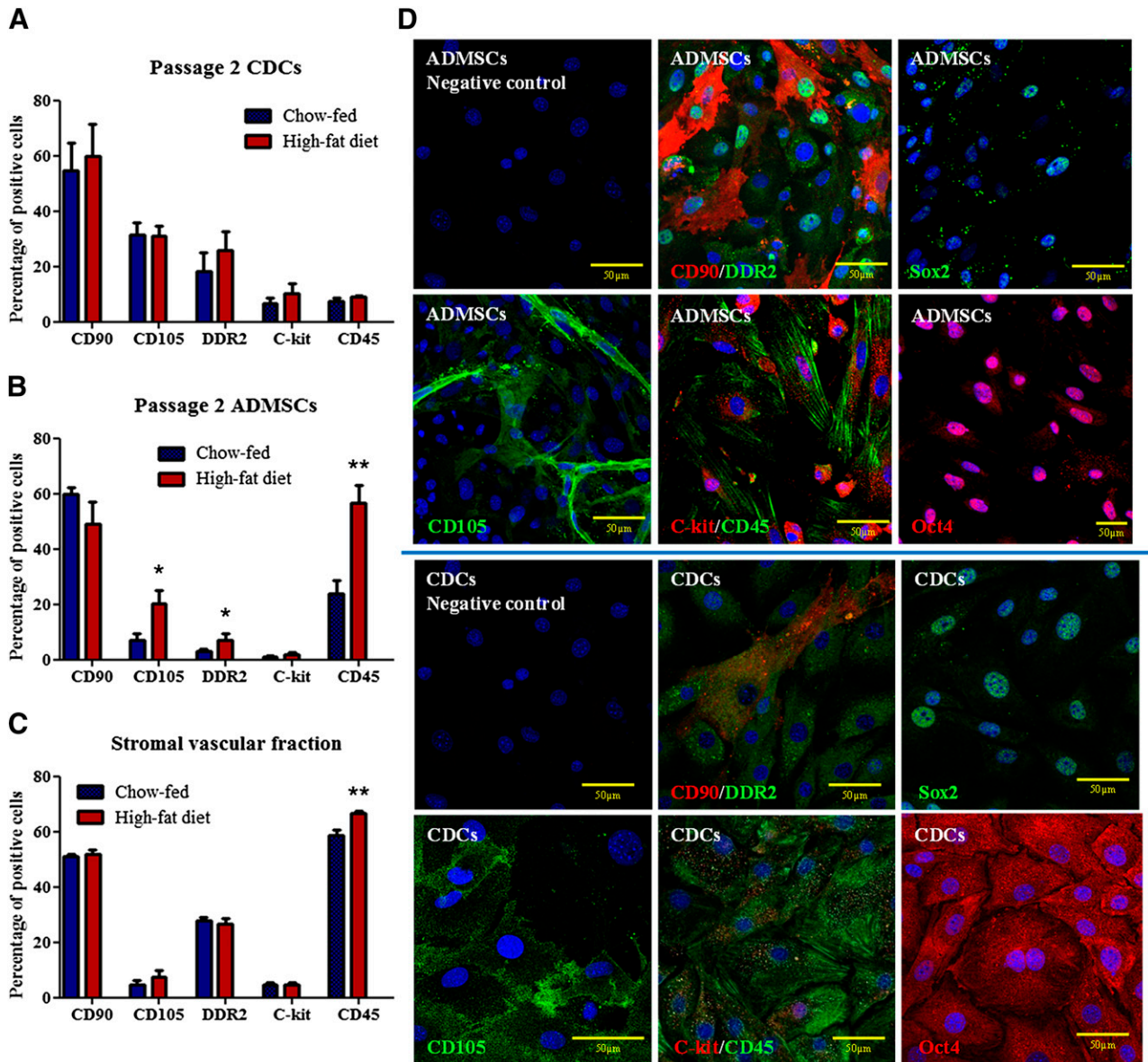
Figure 7. Markers expression of ADMSCs and CDCs. **(A–C):** Flow cytometric analysis showed a higher expression of CD45-positive cells in the stromal vascular fraction from high-fat diet (HFD)-fed mice. Passage 2 ADMSCs were found to express more CD45, CD105, and DDR2 than ADMSCs from chow-fed mice. Cell surface marker expression did not differ between CDCs from chow-fed and HFD-fed mice ($n = 10$). **(D):** Representative confocal images showed that most of the CDCs were positive for Oct4 and Sox2 (green), weakly positive for CD45 (green), CD105 (green), C-kit (red), and DDR2 (green), and some cells were highly positive for CD90 (red). Nuclei were counterstained with 4′,6-diamino-2-phenylindole (blue). Scale bar = 50 μm. ∗, $p < .05$; ∗, $p < .01$ ($n = 11$). Abbreviations: ADMSCs, adipose-derived mesenchymal cells; CDCs, cardiosphere-derived cells.

amount of VEGF protein accumulated in the culture medium of CDCs, irrespective of mouse diet. In medium from ADMSCs from HFD-fed mice, the levels of VEGF were lower, although not significantly so, and this suggests an impaired ability of these cells to produce and release angiogenic mediators. It is likely that a more severe diabetic state would have increased the difference between the two groups. We then evaluated the migratory capacity of the cells. It was not possible to perform this experiment with CDCs because of insufficient cell numbers. No differences were noticed between ADMSCs from the two groups, which suggests a similar migratory capacity. We also evaluated the clonogenic capacity of ADMSCs and CDCs, and we found that ADMSCs have a low clonogenic capacity and that the number of colonies decreased with time in culture. Similar results have been shown

before with prolonged in vitro culture of mesenchymal cells [35]. In comparison, CDCs showed a higher clonogenic capacity, which increased between passage 0 and passage 2. Several different types of colonies were noticed with high variability of cell morphologies between colonies, most likely because of heterogeneity of progenitor cell types within the CDCs population. Interestingly, the increase in the clonogenic capacity matched the decreased doubling time in later passage CDCs. ADMSCs and CDCs from chow-fed and HFD-fed mice were characterized using flow cytometry and confocal microscopy, with staining for markers of progenitor cells, fibroblasts, mesenchymal cells, and hematopoietic cells. The results showed that the cells displayed a mesenchymal/fibroblast phenotype with low expression of the cardiac progenitor cell markers.

The cells of the SVF included a range of cell types, mostly expressing the mesenchymal, fibroblast, and hematopoietic markers CD90, DDR2, and CD45, respectively. The only difference found between the two diet groups was higher expression of CD45 in HFD SVF, which could be justified by an infiltration of hematopoietic cells in the adipose tissue as previously reported [28, 29]. However, after in vitro expansion, passage 3 ADMSCs from HFD-fed mice displayed a different phenotype compared with those from chow-fed mice, with higher levels of CD105, DDR2, and CD45. Other groups have previously described an increase of CD105+ cells in cultured ADMSCs [36, 37]. Jing et al. [38] demonstrated that in a coculture system, hematopoietic cells can improve proliferation if associated with mesenchymal stromal cells. We can assume that the differences in surface marker expression of ADMSCs from HFD-fed mice may be explained by the in vitro culture conditions, that could have had an effect in maintaining and allowing these various cell populations to survive and/or proliferate. Although most of the CDCs and ADMSCs expressed mesenchymal and fibroblast maskers, the detection of progenitor/pluripotency markers suggest the presence of progenitor cells within these two cell populations. In this study, cells were treated with differentiation medium containing 5-azacytidine + TGFβ or Methocult + Noggin because, from previous experiments (data not shown), these protocols were able to induce a better differentiation along the cardiomyocyte lineage. No differences were noticed in the differentiation potential of CDCs from chow-fed and HFD-fed mice, that further confirms the conclusion that the high-fat diet does not affect cardiac progenitor cells. In a recent study, we showed that CDCs isolated from mice aged 6 and 18 months had the same number and regenerative potential, whether from dystrophic mice, with mild cardiac impairment, or from age-matched wild-type mice [39]. The differentiation of ADMSCs increased expression levels of cardiac genes; however, ADMSCs from HFD-fed mice seemed to have a slower response to the induction of differentiation. Troponin T increased later in the differentiation protocol and had lower expression compared with that in ADMSCs from chow-fed animals, whereas genes expressed earlier in differentiation (such as Gata4 and Desmin) were higher in the differentiated ADMSCs from HFD-fed mice. We suggest that the reduced differentiation capacity of ADMSCs from HFD-fed mice could be due to the higher percentage of hematopoietic cells, which are reported to be less likely to differentiate into cardiomyocytes than mesenchymal cells [40–42]. The lack of troponin T and α actinin (sarcomeric) signal from both CDCs and ADMSCs suggests that the amount of protein produced was not enough to be detected from the antibodies, further confirming the early stage of differentiation achieved. The increased levels of actin suggest a general effect of the TGFβ-supplemented medium on the cytoskeleton organization of these cells. SMA has been identified as an important marker for the identification of cardiac fibroblasts [43], and it has been shown that TGFβ is one of the driving factors for the differentiation of cardiac fibroblasts into myofibroblasts [44]. These cells are involved in the scar formation and particularly involved in the deposition of collagen and extracellular matrix after myocardial infarction [44–46]. The increase in the number of SMA-positive cells after treatment with TGFβ differentiation medium is probably due to the proliferation of the fibroblasts still present in the heterogeneous population that form both ADMSCs and CDCs. Because TGFβ is upregulated after myocardial infarction [47], this suggests that it may be important to isolate cells in such a way that the number of fibroblasts present after in vitro expansion is reduced. In summary, both ADMSCs and CDCs increased the expression of cardiac specific genes; however, no beating cells were observed, indicating that the cells did not acquire the phenotype of fully mature cardiomyocytes.

CONCLUSION

Here we investigated the effect of a HFD on mesenchymal cells from cardiac and adipose tissues. The HFD altered various metabolic pathways, thereby creating a mouse model of early stage type 2 diabetes. Heart tissue explant culture yielded sufficient CDCs for therapy, although this required substantial in vitro expansion. From adipose tissue from HFD-fed mice, it was possible to isolate a greater number of ADMSCs than from that from chow-fed mice; however, the early diabetic phenotype modified the surface marker expression profile of ADMSCs and their differentiation capacity. CDCs were not affected by the early diabetic phenotype, suggesting that they may be a better candidate for cell therapy.

AUTHOR CONTRIBUTIONS

F.P.: conception and design, collection and assembly of data, data analysis and interpretation, manuscript writing, final approval of manuscript; R.S.M.G.: conception and design, collection and assembly of data, data analysis and interpretation; S.V., D.B., S.M.-M., A.A.N.B., M.d.L.S.F., and V.B.: collection and assembly of data; K.C.: conception and design, financial support; G.F.: financial support; C.A.C.: conception and design, collection and assembly of data, data analysis and interpretation, manuscript writing.

DISCLOSURE OF POTENTIAL CONFLICTS OF INTEREST

The authors indicated no potential conflicts of interest.

REFERENCES

1 Pradeepa R, Prabhakaran D, Mohan V. Emerging economies and diabetes and cardiovascular disease. Diabetes Technol Ther 2012; 14(suppl 1):S59–S67.

2 Jawad H, Ali NN, Lyon AR et al. Myocardial tissue engineering: A review. J Tissue Eng Regen Med 2007;1:327–342.

3 Gersh BJ, Simari RD, Behfar A et al. Cardiac cell repair therapy: A clinical perspective. Mayo Clin Proc 2009;84:876–892.

4 Kreutziger KL, Murry CE. Engineered human cardiac tissue. Pediatr Cardiol 2011;32: 334–341.

5 Bonen A, Tandon NN, Glatz JFC et al. The fatty acid transporter FAT/CD36 is upregulated in subcutaneous and visceral adipose tissues in human obesity and type 2 diabetes. Int J Obes (Lond) 2006;30:877–883.

6 Hafstad AD, Solevåg GH, Severson DL et al. Perfused hearts from type 2 diabetic (db/db) mice show metabolic responsiveness to insulin. Am J Physiol Heart Circ Physiol 2006;290:H1763–H1769.

7 Stanley WC, Lopaschuk GD, McCormack JG. Regulation of energy substrate metabolism in the diabetic heart. Cardiovasc Res 1997;34:25–33.

8 Jéquier E. Effect of lipid oxidation on glucose utilization in humans. Am J Clin Nutr 1998;67(suppl):527S–530S.

9 Holness MJ, Kraus A, Harris RA et al. Targeted upregulation of pyruvate dehydrogenase kinase (PDK)-4 in slow-twitch skeletal muscle underlies the stable modification of the regulatory characteristics of PDK induced by high-fat feeding. Diabetes 2000;49:775–781.

10 Bajotto G, Murakami T, Nagasaki M et al. Downregulation of the skeletal muscle pyruvate dehydrogenase complex in the Otsuka Long-Evans Tokushima Fatty rat both before and after the onset of diabetes mellitus. Life Sci 2004;75:2117–2130.

11 Tepper OM, Carr J, Allen RJ Jr et al. Decreased circulating progenitor cell number and failed mechanisms of stromal cell-derived factor-1alpha mediated bone marrow mobilization impair diabetic tissue repair. Diabetes 2010;59:1974–1983.

12 Tepper OM, Galiano RD, Capla JM et al. Human endothelial progenitor cells from type II diabetics exhibit impaired proliferation, adhesion, and incorporation into vascular structures. Circulation 2002;106:2781–2786.

13 Gutiérrez E, Sanz-Ruiz R, Alvarez EV et al. General overview of the Seventh International Symposium on Stem Cell Therapy and Cardiovascular Innovations. J Cardiovasc Transl Res 2011;4:115–120.

14 Makkar RR, Smith RR, Cheng K et al. Intracoronary cardiosphere-derived cells for heart regeneration after myocardial infarction (CADUCEUS): A prospective, randomised phase 1 trial. Lancet 2012;379:895–904.

15 Hsueh W, Abel ED, Breslow JL et al. Recipes for creating animal models of diabetic cardiovascular disease. Circ Res 2007;100:1415–1427.

16 Smits AM, van Vliet P, Metz CH et al. Human cardiomyocyte progenitor cells differentiate into functional mature cardiomyocytes: An in vitro model for studying human cardiac physiology and pathophysiology. Nat Protoc 2009;4:232–243.

17 Jumabay M, Zhang R, Yao Y et al. Spontaneously beating cardiomyocytes derived from white mature adipocytes. Cardiovasc Res 2010;85:17–27.

18 Winzell MS, Ahrén B. The high-fat diet-fed mouse: A model for studying mechanisms and treatment of impaired glucose tolerance and type 2 diabetes. Diabetes 2004;53(suppl 3):S215–S219.

19 Panagia M, Schneider JE, Brown B et al. Abnormal function and glucose metabolism in the type-2 diabetic db/db mouse heart. Can J Physiol Pharmacol 2007;85:289–294.

20 Belke DD, Larsen TS, Gibbs EM et al. Altered metabolism causes cardiac dysfunction in perfused hearts from diabetic (db/db) mice. Am J Physiol Endocrinol Metab 2000;279:E1104–E1113.

21 Brand MD. The efficiency and plasticity of mitochondrial energy transduction. Biochem Soc Trans 2005;33:897–904.

22 Yang D, Wang W, Li L et al. The relative contribution of paracine effect versus direct differentiation on adipose-derived stem cell transplantation mediated cardiac repair. PLoS One 2013;8:e59020.

23 Bai X, Yan Y, Song Y-H et al. Both cultured and freshly isolated adipose tissue-derived stem cells enhance cardiac function after acute myocardial infarction. Eur Heart J 2010;31:489–501.

24 Bolli R, Chugh AR, D'Amario D et al. Cardiac stem cells in patients with ischaemic cardiomyopathy (SCIPIO): Initial results of a randomised phase 1 trial. Lancet 2011;378:1847–1857.

25 Smith RR, Barile L, Cho HC et al. Regenerative potential of cardiosphere-derived cells expanded from percutaneous endomyocardial biopsy specimens. Circulation 2007;115:896–908.

26 Smits AM, van Laake LW, den Ouden K et al. Human cardiomyocyte progenitor cell transplantation preserves long-term function of the infarcted mouse myocardium. Cardiovasc Res 2009;83:527–535.

27 Jain M, DerSimonian H, Brenner DA et al. Cell therapy attenuates deleterious ventricular remodeling and improves cardiac performance after myocardial infarction. Circulation 2001;103:1920–1927.

28 Weisberg SP, McCann D, Desai M et al. Obesity is associated with macrophage accumulation in adipose tissue. J Clin Invest 2003;112:1796–1808.

29 Makki K, Froguel P, Wolowczuk I. Adipose tissue in obesity-related inflammation and insulin resistance: Cells, cytokines, and chemokines. ISRN Inflamm 2013;2013:139239.

30 McLaughlin T, Deng A, Gonzales O et al. Insulin resistance is associated with a modest increase in inflammation in subcutaneous adipose tissue of moderately obese women. Diabetologia 2008;51:2303–2308.

31 Pérez LM, Bernal A, San Martín N et al. Obese-derived ASCs show impaired migration and angiogenesis properties. Arch Physiol Biochem 2013;119:195–201.

32 Oñate B, Vilahur G, Ferrer-Lorente R et al. The subcutaneous adipose tissue reservoir of functionally active stem cells is reduced in obese patients. FASEB J 2012;26:4327–4336.

33 Rota M, Padin-Iruegas ME, Misao Y et al. Local activation or implantation of cardiac progenitor cells rescues scarred infarcted myocardium improving cardiac function. Circ Res 2008;103:107–116.

34 Leonardini A, Avogaro A. Abnormalities of the cardiac stem and progenitor cell compartment in experimental and human diabetes. Arch Physiol Biochem 2013;119:179–187.

35 Briquet A, Dubois S, Bekaert S et al. Prolonged ex vivo culture of human bone marrow mesenchymal stem cells influences their supportive activity toward NOD/SCID-repopulating cells and committed progenitor cells of B lymphoid and myeloid lineages. Haematologica 2010;95:47–56.

36 Lin C-S, Xin Z-C, Deng C-H et al. Defining adipose tissue-derived stem cells in tissue and in culture. Histol Histopathol 2010;25:807–815.

37 Mitchell JB, McIntosh K, Zvonic S et al. Immunophenotype of human adipose-derived cells: Temporal changes in stromal-associated and stem cell-associated markers. STEM CELLS 2006;24:376–385.

38 Jing D, Fonseca A-V, Alakel N et al. Hematopoietic stem cells in co-culture with mesenchymal stromal cells: Modeling the niche compartments in vitro. Haematologica 2010;95:542–550.

39 Hsiao L-C, Perbellini F, Gomes RSM et al. Murine cardiosphere-derived cells are impaired by age but not by cardiac dystrophic dysfunction. Stem Cells Dev 2014;23:1027–1036.

40 Murry CE, Soonpaa MH, Reinecke H et al. Haematopoietic stem cells do not transdifferentiate into cardiac myocytes in myocardial infarcts. Nature 2004;428:664–668.

41 Nygren JM, Jovinge S, Breitbach M et al. Bone marrow-derived hematopoietic cells generate cardiomyocytes at a low frequency through cell fusion, but not transdifferentiation. Nat Med 2004;10:494–501.

42 Fukuda K, Fujita J. Mesenchymal, but not hematopoietic, stem cells can be mobilized and differentiate into cardiomyocytes after myocardial infarction in mice. Kidney Int 2005;68:1940–1943.

43 Camelliti P, Borg TK, Kohl P. Structural and functional characterisation of cardiac fibroblasts. Cardiovasc Res 2005;65:40–51.

44 Zeisberg EM, Kalluri R. Origins of cardiac fibroblasts. Circ Res 2010;107:1304–1312.

45 Leask A, Abraham DJ. TGF-beta signaling and the fibrotic response. FASEB J 2004;18:816–827.

46 Chen H, Yang W-W, Wen Q-T et al. TGF-beta induces fibroblast activation protein expression; fibroblast activation protein expression increases the proliferation, adhesion, and migration of HO-8910PM. Exp Mol Pathol 2009;87:189–194; published correction appears in Exp Mol Pathol 2010;88:433.

47 Vilahur G, Juan-Babot O, Peña E et al. Molecular and cellular mechanisms involved in cardiac remodeling after acute myocardial infarction. J Mol Cell Cardiol 2011;50:522–533.

See www.StemCellsTM.com for supporting information available online.